Inhibitive Properties and Adsorption of Purpald as a Corrosion Inhibitor for Copper in Nitric Acid Medium

ARTICLE *in* INDUSTRIAL & ENGINEERING CHEMISTRY RESEARCH · FEBRUARY 2013

Impact Factor: 2.59 · DOI: 10.1021/ie301465k

4 AUTHORS, INCLUDING:

Abdelkader Zarrouk
Université Mohammed Premier
152 PUBLICATIONS **1,028** CITATIONS
SEE PROFILE

Belkheir Hammouti
Université Mohammed Premier
96 PUBLICATIONS **319** CITATIONS
SEE PROFILE

Fouad Bentiss
National Graduate School of Engineering Che…
137 PUBLICATIONS **5,662** CITATIONS
SEE PROFILE

I&EC research
Industrial & Engineering Chemistry Research

Article

pubs.acs.org/IECR

Inhibitive Properties and Adsorption of Purpald as a Corrosion Inhibitor for Copper in Nitric Acid Medium

Abdelkader Zarrouk,[†] Belkheir Hammouti,[†] Ali Dafali,[†] and Fouad Bentiss*[,‡]

[†]Laboratoire de Chimie Appliquée et Environnement, LCAE-URAC18, Faculté des Sciences, Université Mohammed Premier, B.P. 717, M-6000 Oujda, Morocco

[‡]Laboratoire de Chimie de Coordination et d'Analytique (LCCA), Faculté des Sciences, Université Chouaib Doukkali, B.P. 20, M-24000 El Jadida, Morocco

ABSTRACT: Inhibition performance of purpald (4-amino-3-hydrazino-5-mercapto-1,2,4-triazole (AHMT)) was investigated as a corrosion inhibitor for a copper surface in 2 M HNO_3 at 303 K by weight loss, ac impedance, and dc polarization techniques. The obtained results indicate that AHMT is a good inhibitor and its inhibition efficiency attains 94.7% at 10^{-2} M. Polarization studies showed that AHMT acts as a mixed type inhibitor. The inhibitor adsorption process in the Cu/AHMT/2 M HNO_3 system was studied at different temperatures (303−343 K). The adsorption of AHMT on the copper surface obeyed Langmuir's adsorption isotherm. The kinetic and adsorption parameters for copper/acid in the presence and absence of AHMT were evaluated and discussed.

1. INTRODUCTION

Copper is a metal that has a wide range of applications due to its good properties. It is used in electronics, for production of wires, sheets, and tubes, and also to form alloys. The use of copper corrosion inhibitors in acid solutions is usually to minimize the corrosion of copper during the acid cleaning and descaling. The possibility of the copper corrosion prevention has attracted many researchers so until now numerous possible inhibitors have been investigated.[1−8] Heterocyclic compounds such as imidazole, tetrazole, 1,3,4-thiadiazole, benzothiazole, and benzotriazole have been reported to inhibit the corrosion of copper.[9−15] Among the various nitrogen and sulfur compounds studied as inhibitors, triazoles have been considered as environmentally acceptable chemicals. Many substituted triazole compounds have been recently studied in considerable details as effective corrosion inhibitors for steel and copper in acidic media.[13−22] The inhibition of these organic compounds is usually attributed to their interaction with the copper surface via their adsorption. The adsorption of an inhibitor onto a metal surface depends on the nature as well as the surface charge of the metal, the adsorption mode, its chemical structure, and the type of the electrolyte solution.[23]

In continuation of our work on development of 1,2,4-triazole derivatives as inhibitors for corrosion copper in nitric acid medium,[24,25] we have studied the corrosion inhibiting behavior of purpald, namely 4-amino-3-hydrazino-5-mercapto-1,2,4-triazole (AHMT) on copper in 2 M HNO_3 solution using weight loss, ac impedance, and Tafel polarization techniques. The thermodynamic parameters describing the kinetic of corrosion as well as the adsorption process when varying temperature and concentration of AHMT are evaluated and discussed.

2. EXPERIMENTAL DETAILS

The investigated 1,2,4-triazole (purpald), namely 4-amino-3-hydrazino-5-mercapto-1,2,4-triazole (AHMT), is obtained from Sigma-Aldrich Chemical Co., and its chemical structure is presented in Figure 1. The concentration range of the tested inhibitor employed was 1×10^{-5} to 1×10^{-2} M. The solubility of AHMT is slightly greater than 10^{-2} M in 2 M HNO_3.

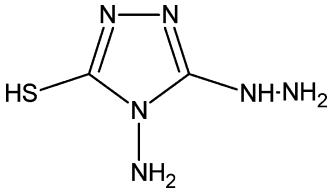

Figure 1. Molecular structure of AHMT.

The material used in this study is a copper with a chemical composition (wt %) of 0.01% Ni, 0.019% Al, 0.004% Mn, 0.116% Si, and 99.5% Cu, Prolabo Chemicals. Prior to all measurements, the copper samples were pretreated by grinding with emery paper SiC (180, 600, and 2000); rinsed with distilled water, degreased in ethanol in an ultrasonic bath immersion for 5 min, washed again with bidistilled water, and then dried at room temperature before use. The acid solutions (2 M HNO_3) were prepared by dilution of an analytical reagent grade 65% HNO_3 with doubly distilled water.

The gravimetric measurements were carried out at the definite time interval of 1 h at room temperature using an analytical balance (precision ±0.1 mg). Each run was carried out in a glass vessel containing 100 mL of the test solution. A clean weighed copper electrode ($2 \times 2 \times 0.2$ cm^3) was completely immersed at inclined position in the vessel. After the exposure time, the electrode was withdrawn, rinsed with

Received: June 5, 2012
Revised: December 19, 2012
Accepted: January 24, 2013
Published: January 24, 2013

   dx.doi.org/10.1021/ie301465k | *Ind. Eng. Chem. Res.* 2013, 52, 2560−2568

doubly distilled water, washed with ethanol, dried, and weighed. Two batches of tests were performed, and the data reported in this paper represent the average value of the two tests. The weight loss (w), in milligrams, was taken as the difference in the weight of the copper coupons before and after immersion in different test solutions. Weight loss allowed calculation of the mean corrosion rate (C_R) in milligrams per squared centimter per hour. The standard deviation of the observed weight loss was ±1%.

Electrochemical measurements were carried out in a conventional three-electrode cylindrical Pyrex glass cell. All electrochemical tests have been performed at 303 K in nondeaerated solutions The working electrode (WE) in the form of disc cut from copper has a geometric area of 0.28 cm^2 and is embedded in polytetrafluoroethylene (PTFE). A saturated calomel electrode (SCE) and a platinum electrode were used, as reference and auxiliary electrodes, respectively. A fine Luggin capillary was placed close to the working electrode to minimize ohmic resistance. The working electrode was immersed in test solution during 30 min until a steady state open circuit potential (E_{ocp}) was obtained.

Electrochemical impedance spectroscopy experiments were conducted using a Tacussel Radiometer PGZ 3O1, and Voltamaster.4 Software was used to run the tests and to collect the experimental data. Alternating current (ac) impedance measurements were carried-out in the frequency range of 100 kHz to 10 mHz, with 10 points per decade, by applying 10 mV ac voltage peak-to-peak. Nyquist plots were made from these experiments.

Potentiodynamic polarization experiments were conducted using an electrochemical measurement system Tacussel Radiometer PGZ 301 controlled by a PC supported by Voltamaster.4 Software. The polarization curve was recorded by polarization from −150 to 150 mV versus E_{ocp} with a scan rate of 1 mV s^{-1} under an air atmosphere.

3. RESULTS AND DISCUSSION

3.1. Corrosion Inhibition Evaluation. *3.1.1. Weight Loss Measurements.* The inhibition effect of the investigated 1,2,4-triazole (AHMT) at different concentrations on the corrosion of copper in 2 M HNO_3 solution was studied by weight loss measurements at 303 K after 1 h of immersion period. The corrosion rate (C_R) and inhibition efficiency, $\eta_{WL}(\%)$, were calculated according to the eqs 1 and 2,[26,27] respectively:

$$C_R = \frac{W_b - W_a}{At} \quad (1)$$

$$\eta_{WL}(\%) = \left(1 - \frac{w_i}{w_0}\right) \times 100 \quad (2)$$

where W_b and W_a are the specimen weight before and after immersion in the tested solution, w_0 and w_i are the values of corrosion weight losses of copper in uninhibited and inhibited solutions, respectively, A is the area of the copper specimen (cm^2), and t is the exposure time (h).

The values of percentage inhibition efficiency (η_{WL} %) and corrosion rate (C_R) obtained from weight loss method at different concentrations of AHMT at 303 K are summarized in Table 1. These results show that the AHMT inhibits the corrosion of copper in 2 M HNO_3 solution, at all concentrations used in this study, and the corrosion rate (C_R) decreases continuously with increasing additive concentration at 303 K. The corrosion rate was found to depend on the concentration of the AHMT and $\eta_{WL}(\%)$ of AHMT increases with concentration increasing, the maximum $\eta_{WL}(\%)$ of 91.7% is achieved at 10^{-2} M. The corrosion resistance of copper steel in 2 M HNO_3 by other 1,2,4-triazole derivatives was previously described in the same conditions.[24,25] At the same concentration (10^{-2} M), the inhibition efficiency attains 82.2% and 86.5% for 3-amino-1,2,4-triazole (ATA)[24] and 3,5-diamino-1,2,4-triazole (DAT),[25] respectively. Thus, we can deduce that AHMT is the best inhibitor of this family and the inhibition efficiency was found to be in the following order AHMT > DAT > ATA. The variation in inhibitive efficiency mainly depends on the type and the nature of the substituent of the 1,2,4-triazole moiety. This behavior can be explained by the presence of the mercapto group in the structure of AHMT molecule that perhaps plays an important role in increasing its adsorption probability on the copper surface. This can be explained on the basis that sulfur containing compounds self-assemble on the copper surface by forming strong covalent bonds between the sulfur atoms and the metal surface.[28−30] This behavior is in agreement with the literature.[17]

Table 1. Corrosion Parameters Obtained from Weight Loss Measurements for Copper in 2 M HNO_3 Containing Various Concentrations of AHMT at 303 K

C_{inh} (M)	C_R (mg cm^{-2} h^{-1})	η_{WL} (%)
blank	1.780	
1×10^{-5}	1.186	33.4
5×10^{-5}	1.120	37.1
1×10^{-4}	0.846	52.5
5×10^{-4}	0.741	58.3
1×10^{-3}	0.454	74.5
5×10^{-3}	0.215	87.9
1×10^{-2}	0.147	91.7

The plausible mechanism for corrosion inhibition of copper in 2 M HNO_3 by AHMT may be explained on the basis of adsorption behavior, which limits the dissolution of the latter by blocking of its corrosion sites and hence decreasing the corrosion rate, with increasing efficiency as their concentrations increase. In acidic solutions, the 1,2,4-triazole molecules exist as cations ($AHMTH^+$) and adsorb through electrostatic interactions between the positively charged AHMT cations.[31] Owing to the acidity of the medium, AHMT molecules can exist as a neutral species or in the cationic form. Thus, the neutral AHMT can be adsorbed by the interaction between the lone pairs of electrons of the nitrogen and sulfur atoms with the copper surface, involving the displacement of water molecules from the metal surface. This processes facilitated by the presence of d vacant orbitals of low energy in the copper ions, as observed in transition group metals. Moreover, the presence of the electron releasing character of the −SH group may be attributed to the increased electron density leading to electron transfer mechanism from functional group to metal surface. In order to obtain a better understanding of the corrosion protection mechanism of AHMT against the corrosion of copper in 2 M HNO_3 medium, a detailed study on this inhibitor was carried out using ac impedance, Tafel polarization, and thermodynamic studies.

3.1.2. Alternating Current Impedance Study. To obtain a better understanding of interaction mechanism between AHMT molecules and copper surface in 2 M HNO_3, electrochemical impedance spectroscopy measurements in the

dx.doi.org/10.1021/ie301465k | Ind. Eng. Chem. Res. 2013, 52, 2560−2568

range of 100 kHz to 10 mHz at open circuit potential were carried out. The impedance behavior of copper in HNO_3 solutions is somewhat similar to that of copper in H_2SO_4 and HCl solutions.[32] The anodic dissolution of copper in the halide-containing solutions has been proved to be diffusion limited.[33] The diffusion step was due to the transport of CuX^{2-} to the bulk solution.[34] However, the corrosion reaction of copper in halide solutions at E_{corr} is composed of the oxidation of copper and the reduction of oxygen dissolved in the solutions;[35] these two half reactions also expected to occur in aerated HNO_3 solutions.

Figure 2 shows the impedance spectra of copper obtained at open-circuit potential after an exposure period of 30 min in 2

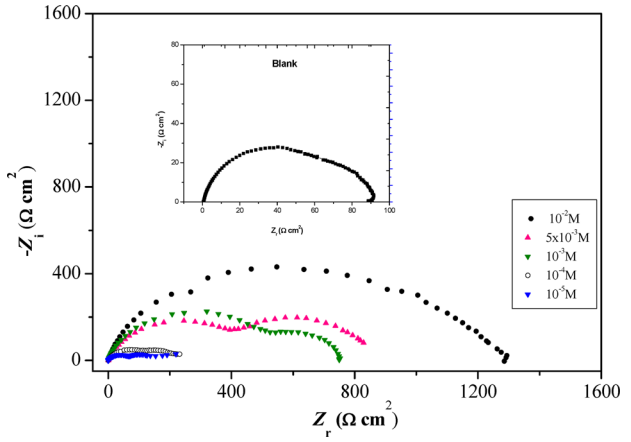

Figure 2. Nyquist diagrams for copper in 2 M HNO_3 containing different concentrations of AHMT at 303 K.

M HNO_3 solution in the absence and presence of different concentrations of AHMT at 303 K. The recorded impedance spectra are, in all cases, characterized by the appearance of two clearly resolved time constants related to the both capacitive loops, the first loop in high frequency (HF) range, and the second one in the low frequency (LF) range. The first capacitive loop can be related to charge-transfer in the corrosion process.[36] The depressed form of the higher frequency loop reflects the surface inhomogeneity of structural or interfacial origin, such as those found in adsorption processes.[37] The presence of the second capacitive loop may be attributed to the adsorption of inhibitor molecules on the metal surface and/or all other accumulated species at the metal/solution interface (inhibitor molecules, corrosion products, etc.).[38]

The analysis of Figure 2 shows that AHMT inhibits the nitric acid corrosion of copper. Indeed, the presence of AHMT increases the impedance (i.e., size of the capacitive loop) with increasing of inhibitor concentration. The increase in the size of the capacitive loop with the addition of AHMT molecules show that a barrier gradually forms on the copper surface. The barrier is probably related to the formation of an inhibitor surface film through its adsorption on the copper surface.

It is well-known that it is essential to develop the appropriate models for the impedance which can then be used to fit the experimental data and extract the parameters which characterize the corrosion process. Indeed, we tried with many suggested equivalent circuits to fit our impedance data using ZView 2.80 equivalent circuit software. Unfortunately, we failed to get a good fitting with our results. It seems that our impedance data are rather complicated (may be due to the formation of two time constants) and require further investigation, in a separate paper, to get the suitable equivalent circuits. For these reasons, the total resistance (polarization resistance, R_p) values are calculated from the difference in impedance at lower and higher frequencies, as suggested by Tsuru et al.,[39] using a nonlinear least-squares fit "fit circle option" (Table 2). The related

Table 2. Impedance Parameters and Inhibition Efficiency Values for Copper in 2 M HNO_3 Containing Different Concentrations of AHMT at 303 K

C_{inh} (M)	R_p (Ω cm^2)	η_Z (%)
blank	91.4	
1×10^{-5}	157.6	42.0
1×10^{-4}	232.7	60.7
1×10^{-3}	759.7	88.0
5×10^{-3}	900.0	89.8
1×10^{-2}	1276.0	92.8

inhibition efficiency, $\eta_Z(\%)$, is calculated from R_p using the following equation:

$$\eta_Z(\%) = \frac{R_{p(i)} - R_p}{R_{p(i)}} \times 100 \quad (3)$$

where R_p and $R_{p(i)}$ are the ac polarization resistance of copper electrode in the uninhibited and inhibited solutions, respectively.

The analysis of the electrochemical parameters shows that the R_p value increases when the AHMT concentration increases, giving consequently a decrease in the corrosion rate. The inhibition efficiency $\eta_Z(\%)$ is also found to increase with the concentration of AHMT, reaching its maximum value at 10^{-2} M. Thus, ac impedance study confirms the inhibiting nature of AHMT and the inhibition efficiencies values, calculated from this method, show the same trend as those obtained from weight loss measurements.

3.1.3. Potentiodynamic Polarization Study. Polarization measurements have been carried out in order to gain knowledge concerning the kinetics of the anodic and cathodic reactions. The potentiodynamic polarization curves for copper in 2 M HNO_3 solutions without and with addition of different concentrations of AHMT at 303 K are shown in Figure 3. Being

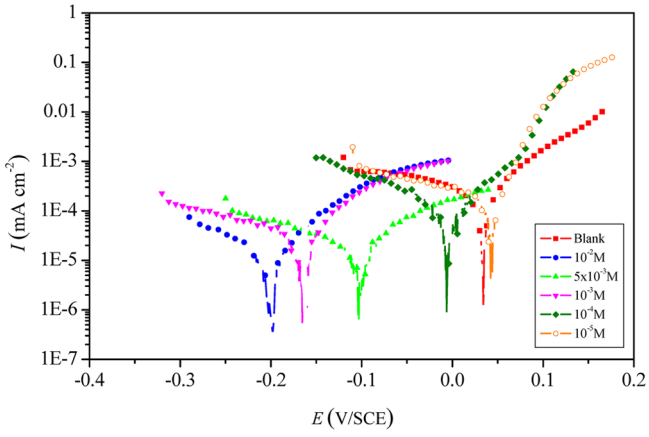

Figure 3. Typical polarization curves for copper in 2 M HNO_3 for various concentrations of AHMT at 303 K.

dx.doi.org/10.1021/ie301465k | Ind. Eng. Chem. Res. 2013, 52, 2560−2568

a strong oxidizing agent, HNO_3 is capable of attacking copper. The Tafel polarization curves exhibit no steep slope in the anodic range, which proves that no passive film is formed on the copper surface. As a result, copper may directly dissolve in 2 M HNO_3 solution. On the basis of the known Pourbaix diagram for a copper−water system, copper is oxidized to Cu^{2+} in 2 M HNO_3 solutions, and no oxide film is formed to protect the surface from the attack of the corrosive medium. Copper dissolution is thus expected to be the dominant reaction in HNO_3 solution.[40]

The anodic and cathodic current−potential curves are extrapolated up to their intersection at a point where corrosion current density (I_{corr}) and corrosion potential (E_{corr}) are obtained.[41] Table 3 shows the electrochemical parameters (I_{corr}, E_{corr}, and b_c) obtained from Tafel plots for the copper electrode in 2 M HNO_3 without and with different concentrations of the investigated 1,2,4-triazole derivative (AHMT). The I_{corr} values were used to calculate the inhibition efficiency, $\eta_{Tafel}(\%)$ (listed in Table 3), using the following equation:[42]

Table 3. Polarization Parameters and the Corresponding Inhibition Efficiency of Copper Corrosion in 2 M HNO_3 Containing Different Concentrations of AHMT at 303 K

C_{inh} (M)	E_{corr} (mV/SCE)	β_c (mV dec^{-1})	I_{corr} (μA cm^{-2})	η_{Tafel} (%)
blank	34	238	365	
1×10^{-5}	43	203	202	44.6
1×10^{-4}	−1	143	149	59.3
1×10^{-3}	−165	219	38	89.7
5×10^{-3}	−103	164	28	92.2
1×10^{-2}	−200	164	20	94.7

$$\eta_{Tafel}(\%) = \frac{I_{corr} - I_{corr(i)}}{I_{corr}} \times 100 \quad (4)$$

where I_{corr} and $I_{corr(i)}$ are the corrosion current densities for copper electrode in the uninhibited and inhibited solutions, respectively.

Inspection of the Figure 3 shows that AHMT has an inhibitive effect in the both anodic and cathodic parts of the polarization curves and the addition of AHMT shifted the E_{corr} value toward the negative direction compared to the uninhibited copper. These findings mean that the inhibitor molecules are adsorbed on both the anodic and cathodic sites, retarding both anodic dissolution and cathodic reduction reactions. For copper corrosion in aerated acidic solutions at E_{corr}, the anodic reaction is copper dissolution and cathodic reaction is oxygen reduction being the hydrogen discharge current density negligible as compared to oxygen reduction current density.[43] More details concerning the electrochemical reactions for copper in aerated nitric solutions are present in our previous study.[24] So, it could be concluded that this 1,2,4-triazole derivative (AHMT) is of the mixed-type for copper in 2 M HNO_3 solution. Indeed, this inhibitor can exist as a cationic species in 2 M HNO_3 medium, which may be adsorbed on the cathodic sites of the copper and retard the oxygen evolution reaction. Moreover, the adsorption of this compound on the anodic sites of copper surface through the lone pairs of electrons of nitrogen and/or sulfur atoms will then reduce the copper dissolution process.

The analyze of the data in Table 3 revealed that the corrosion current density (I_{corr}) decreases considerably with increasing AHMT concentration, while a clear trend was observed in the evolution of E_{corr} values. The cathodic Tafel slope (β_c) values show slight changes with the addition of AHMT, which suggests that the inhibiting action occurred by simple blocking of the available cathodic sites on the metal surface, which lead to a decrease in the exposed area necessary for oxygen reduction and lowered the dissolution rate with increasing AHMT concentration. The dependence of protection efficiency $\eta_{Tafel}(\%)$ versus the inhibitor concentration of AHMT is also presented in Table 3. The obtained inhibition efficiencies indicate that this 1,2,4-triazole acts as effective inhibitor and $\eta_{Tafel}(\%)$ increases as AHMT concentration increases, reaching its maximum value at 10^{-2} M (94.7%). The obtained results by the dc polarization study are in acceptable agreement with those obtained from weight loss and ac impedance studies.

3.2. Effect of Temperature. *3.2.1. Thermodynamic Activation Parameters.* The effect of temperature on the inhibited acid−metal reaction is very complex, because many changes occur on the metal surface such as rapid etching, desorption of inhibitor, and the inhibitor itself may undergo decomposition.[44] The change of the corrosion rate at selected concentrations of the AHMT during 1 h of immersion with the temperature was studied in 2 M HNO_3, both in absence and presence of AHMT. For this purpose, gravimetric experiments were performed at different temperatures (303−343 K). The fractional surface coverage θ can be easily determined from weight loss measurements by the ratio $\eta_{WL}(\%)/100$, if one assumes that the values of $\eta_{WL}(\%)$ do no differ substantially from θ. It is clear from Table 4 that the increase of corrosion rate (C_R) is more pronounced with the rise of temperature for blank solution. In the presence of the AHMT molecule, the corrosion rate of copper decreases at any given temperature as

Table 4. Corrosion Parameters Obtained from Weight Loss for Copper in 2 M HNO_3 Containing Various Concentrations of AHMT at Different Temperatures

temperature (K)	C_{inh} (M)	C_R (mg cm^{-2} h^{-1})	η_{WL} (%)	θ
303	blank	1.78		
	5×10^{-4}	0.741	58.3	0.583
	1×10^{-3}	0.454	74.5	0.745
	5×10^{-3}	0.215	87.9	0.879
	1×10^{-2}	0.147	91.7	0.917
313	Blank	7.33		
	5×10^{-4}	3.983	45.7	0.457
	1×10^{-3}	2.969	59.5	0.595
	5×10^{-3}	1.780	79.8	0.798
	1×10^{-2}	1.164	79.2	0.792
323	blank	24.97		
	5×10^{-4}	14.241	43.1	0.431
	1×10^{-3}	11.668	53.2	0.532
	5×10^{-3}	6.740	71.4	0.714
	1×10^{-2}	5.365	74.3	0.743
333	blank	70.82		
	5×10^{-4}	43.513	38.6	0.386
	1×10^{-3}	35.078	50.5	0.505
	5×10^{-3}	24.368	65.6	0.656
	1×10^{-2}	22.912	67.7	0.677
343	blank	186.61		
	5×10^{-4}	133.848	28.3	0.283
	1×10^{-3}	111.572	40.2	0.402
	5×10^{-3}	85.682	54.1	0.541
	1×10^{-2}	80.438	57.0	0.570

dx.doi.org/10.1021/ie301465k | Ind. Eng. Chem. Res. 2013, 52, 2560−2568

inhibitor concentration increases due to the increase of the degree of surface coverage. In contrast, at constant inhibitor concentration, the corrosion rate increases as temperature rises. Hence we note that the efficiency depends on the temperature and decreases with the rise of temperature from 303 to 343 K. This can be explained by the decrease of the strength of the adsorption process at elevated temperature and would suggest a physical adsorption mode. The inhibition properties of AHMT can also be explained by kinetic model. The activation thermodynamic parameters of the corrosion process were calculated from Arrhenius eq 5 and transition state eq 6:[45]

$$C_R = k \exp\left(-\frac{E_a}{RT}\right) \quad (5)$$

$$C_R = \frac{RT}{Nh} \exp\left(\frac{\Delta S_a}{R}\right) \exp\left(-\frac{\Delta H_a}{RT}\right) \quad (6)$$

where E_a is the apparent activation corrosion energy, R is the universal gas constant, k is the Arrhenius pre-exponential factor, h is Plank's constant, N is Avogrado's number, ΔS_a is the entropy of activation, and ΔH_a is the enthalpy of activation.

Arrhenius plots for the corrosion rate of copper are given in Figure 4. Values of apparent activation energy of corrosion (E_a)

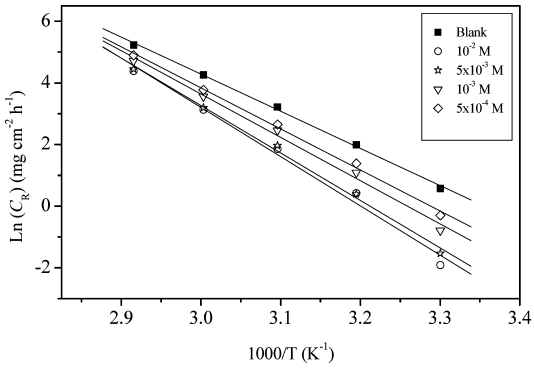

Figure 4. Arrhenius plots for copper corrosion rates (C_R) in 2 M HNO_3 in absence and in presence of different concentrations of AHMT.

for copper in 2 M HNO_3 with the absence and presence of various concentrations of AHMT were determined from the slope of $\ln(C_R)$ vs $1/T$ plots and shown in Table 5. From these findings, we can see that the E_a increases with increasing concentration of AHMT, and all values of E_a in the range of the studied concentration are higher than those in the absence of AHMT. The tendency of variation in pre-exponential factor (A) is similar to that in apparent activation energy. This type of inhibitor retards corrosion at ordinary temperatures but inhibition is diminished at elevated temperature (Table 4). The experimental fact that the activation energy is higher in the presence of inhibitor is explained in different ways in literature.

According to Riggs and Hurd,[46] the decrease in apparent activation energy at higher levels of inhibition arises from a shift of the net corrosion reaction, from one on the uncovered surface to one directly involving the adsorbed sites. This also reveals that the entire process is surface-reaction controlled, since the energy of activation for the corrosion process, both in the absence and presence of inhibitor, was greater than 20 kJ mol^{-1}.[47] Szauer et al. explained that the increase in activation energy can be attributed to an appreciable decrease in the adsorption of the inhibitor on the copper surface with increase in temperature.[48] As adsorption decreases more desorption of inhibitor molecules occurs because these two opposite processes are in equilibrium. Due to more desorption of inhibitor molecules at higher temperatures the greater surface area of copper comes in contact with aggressive environment, resulting in an increase of corrosion rates with temperature. Using high inhibitor concentrations this problem is avoided, because the coverage degrees are close to saturation. The increase in activation energy after the addition of the inhibitor to the 2 M HNO_3 solution can indicate that physical adsorption (electrostatic) occurs in the first stage.[49] Indeed, AHMT molecules are organic bases which are easily protonated to form cationic forms in acid medium. It is logical to assume that in this case the electrostatic cation adsorption is responsible for the good protective properties of this compound. However, the adsorption phenomenon of an organic molecule is not considered only as a physical or as chemical adsorption phenomenon. A wide spectrum of conditions, ranging from the dominance of chemisorption or electrostatic effects, arises from other adsorption experimental data.[50]

Figure 5 shows a plot of $\ln(C_R/T)$ against $1/T$. Straight lines are obtained with a slope of $(-\Delta H_a/R)$ and an intercept of $(\ln R/Nh + \Delta S_a/R)$ from which the values of ΔH_a and ΔS_a are calculated and are listed in Table 5. Inspection of these data

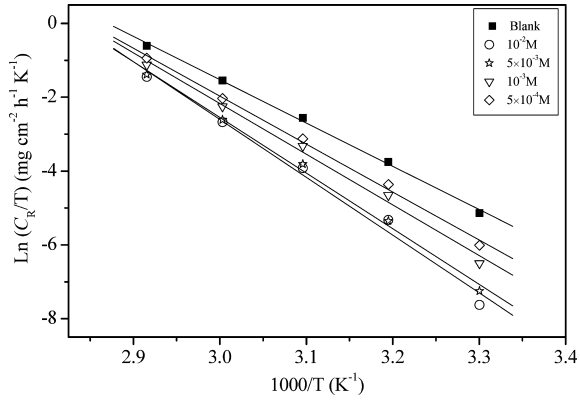

Figure 5. Transition-state plots for copper corrosion rates (C_R) in 2 M HNO_3 in absence and in presence of different concentrations of AHMT.

Table 5. Corrosion Kinetic Parameters for Copper in 2 M HNO_3 at Different Concentrations of AHMT

C_{inh} (M)	k (mg cm^2 h^{-1})	R^2	E_a (kJ mol^{-1})	ΔH_a (kJ mol^{-1})	ΔS_a (J $mol^{-1}K^{-1}$)	$E_a - RT$ (kJ mol^{-1})
blank	3.663×10^{17}	0.999	100.21	97.53	82.36	2.68
5×10^{-4}	1.038×10^{19}	0.998	110.71	108.03	110.16	2.68
1×10^{-3}	7.776×10^{19}	0.997	116.84	114.17	126.90	2.67
5×10^{-3}	3.012×10^{21}	0.998	128.02	125.34	157.31	2.68
1×10^{-2}	1.636×10^{22}	0.994	132.87	130.19	171.38	2.68

dx.doi.org/10.1021/ie301465k | Ind. Eng. Chem. Res. 2013, 52, 2560−2568

reveals that the ΔH_a values for dissolution reaction of copper in 2 M HNO_3 in the presence of AHMT are higher (108.03−130.19 kJ mol^{-1}) than that of in the absence of inhibitors (97.53 kJ mol^{-1}). The positive signs of ΔH_a reflect the endothermic nature of the copper dissolution process suggesting that the dissolution of copper is slow in the presence of inhibitor.[51] The values of E_a and ΔH_a enhance with an increase in the concentration of AHMT suggesting that the energy barrier of corrosion reaction increases as the concentration of AHMT is increased. This means that the corrosion reaction will further be pushed to surface sites that are characterized by progressively higher values of E_a as the concentration of the inhibitor becomes greater.[52] One can also notice that E_a and ΔH_a values vary in the same way. This result permits to verify the known thermodynamic reaction between the E_a and ΔH_a as shown in Table 5:[53]

$$\Delta H_a = E_a - RT \tag{7}$$

ΔS_a increases positively with increasing AHMT concentration (and their values were positive both in the uninhibited and inhibited systems). In addition, the values of ΔS_a were higher for inhibited solutions than that for the uninhibited solution (Table 5). This suggested that an increase in randomness occurred on going from reactants to the activated complex. This might be the results of the adsorption of organic inhibitor molecules from the nitric solution could be regarded as a quasi-substitution process between the organic compound in the aqueous phase and water molecules at electrode surface.[54] In this situation, the adsorption of organic inhibitor was accompanied by desorption of water molecules from the surface. Thus the increasing in entropy of activation was attributed to the increasing in solvent entropy.[55]

3.2.2. Thermodynamic Adsorption Parameters. The adsorption isotherm can be determined if the inhibitor effect is due mainly to the adsorption on the metal surface (i.e., to its blocking). The type of the adsorption isotherms provides information about the interaction among the adsorbed molecules themselves and also their interactions with the electrode surface. The fractional surface coverage θ values are given in Table 4. The experimental data are most often described by the adsorption isotherms of Langmuir, Frumkin, or Temkin. Best fit was obtained with the Langmuir adsorption isotherm:[56]

$$\frac{C_{inh}}{\theta} = \frac{1}{K_{ads}} + C_{inh} \tag{8}$$

where C_{inh} is the inhibitor concentration in the electrolyte and K_{ads} is the equilibrium constant of the adsorption process which is related to the standard Gibbs energy of adsorption, ΔG°_{ads}, according to ref 57

$$K_{ads} = \frac{1}{55.55} \exp\left(\frac{-\Delta G^{\circ}_{ads}}{RT}\right) \tag{9}$$

where R is the universal gas constant, T the thermodynamic temperature, and the value of 55.55 is the concentration of water in the solution in moles per liter. To calculate the adsorption parameters, a least-squares linear optimization procedure was applied. The experimental (points) and calculated isotherms (lines) are plotted in Figure 6. The results are presented in Table 6. A very good fit is observed with the regression coefficients up to 0.999, which suggests that the experimental data are well described by Langmuir isotherm.

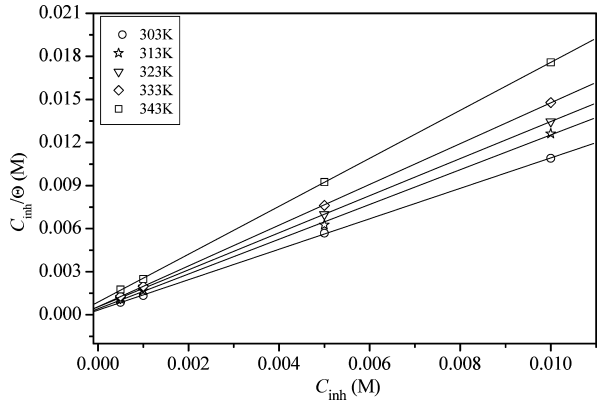

Figure 6. Langmuir's isotherm adsorption model of AHMT on the copper surface in 2 M HNO_3 at different temperatures.

From the intercepts of the straight lines C_{inh}/θ-axis, the K_{ads} values were calculated and given in Table 6. The calculated ΔG°_{ads} values, using eq 8, were also given in Table 6. The obtained values of ΔG°_{ads} show the regular dependence of ΔG°_{ads} on temperature (Table 6), indicating a good correlation among thermodynamic parameters. The large negative values of ΔG°_{ads} ensure the spontaneity of the adsorption process and the stability of the adsorbed layer on the copper surface[58,59] as well as a strong interaction between the AHMT molecules and the metal surface.[60] Generally, absolute values of ΔG°_{ads} up to 20 kJ mol^{-1} are consistent with physisorption, while those around 40 kJ·mol^{-1} or higher are associated with chemisorption as a result of the sharing or transfer of electrons from organic molecules to the metal surface to form a coordinate type of metal bonds.[61] Here, the calculated ΔG°_{ads} values are ranging between −30.38 and −31.83 kJ mol^{-1}. indicating that the adsorption mechanism of AHMT on copper in 2 M HNO_3 solution at the studied temperatures is both electrostatic−adsorption (ionic) and chemisorption (molecular).[62] Indeed, it can be concluded that AHMT can adsorb on the copper surface in two different ways: (i) the AHMT molecule electrostatically adsorbs onto the anion covered metal surface, through its protonated form and (ii) the AHMT molecules compete with acid anions for sites at the water covered surface and the unshared electron pairs in sulfur as well as nitrogen may interact with d-orbitals of copper to provide a protective film.[63]

Thermodynamically, ΔG°_{ads} is related to the standard enthalpy and entropy of the adsorption process, ΔH°_{ads} and ΔS°_{ads}, respectively, via eq 10:

$$\Delta G^{\circ}_{ads} = \Delta H^{\circ}_{ads} - T\Delta S^{\circ}_{ads} \tag{10}$$

and the standard enthalpy of adsorption (ΔH°_{ads}) can be calculated according to the Van't Hoff equation:[64]

$$\ln K_{ads} = -\frac{\Delta H^{\circ}_{ads}}{RT} + \text{constant} \tag{11}$$

A plot of ln K_{ads} versus $1/T$ gives a straight line, as shown in Figure 7. The slope of the straight line is $-\Delta H^{\circ}_{ads}/R$ and the intercept is $[\Delta S^{\circ}_{ads}/R + \ln (1/55.55)]$. The obtained values of ΔH°_{ads} and ΔS°_{ads} are given in Table 6. The values of thermodynamic parameters for the adsorption of inhibitors can provide valuable information about the mechanism of corrosion inhibition. While an endothermic adsorption process ($\Delta H^{\circ}_{ads} > 0$) is attributed unequivocally to chemisorption, an exothermic adsorption process ($\Delta H^{\circ}_{ads} < 0$) may involve

dx.doi.org/10.1021/ie301465k | Ind. Eng. Chem. Res. 2013, 52, 2560−2568

Table 6. Thermodynamic Parameters for the Adsorption of AHMT on the Copper in 2 M HNO_3 at Different Temperatures

temperature (K)	R^2	K_{ads} (M^{-1})	ΔG°_{ads} (kJ mol^{-1})	ΔH°_{ads} (kJ mol^{-1})	ΔS°_{ads} (J mol^{-1} K^{-1})
303	0.999	3113.48	−30.38		
313	0.999	2358.76	−30.66		
323	0.999	1820.00	−30.94	−19.85	34.73
333	0.999	1774.54	−31.83		
343	0.999	1135.54	−31.52		

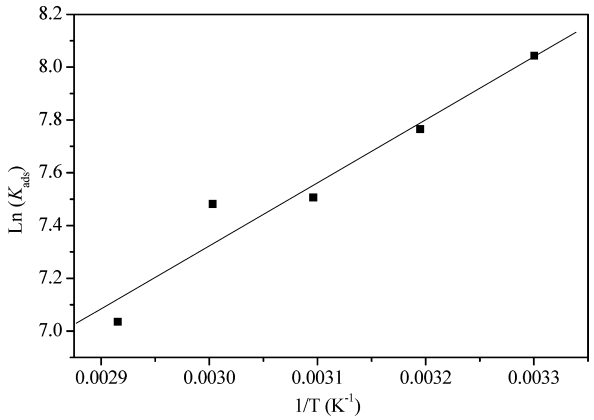

Figure 7. Vant't Hoff plot for the copper/AHMT/2 M HNO_3 system.

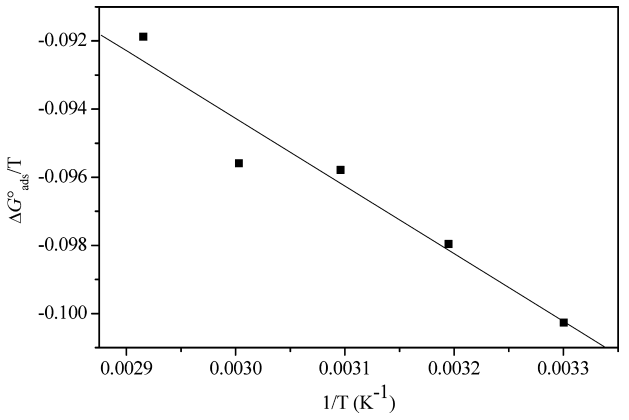

Figure 8. Variation of ΔG°_{ads} versus T on copper in 2 M HNO_3 containing AHMT.

physisorption, chemisorption, or a mixture of both.[65] In an exothermic process, physisorption can be distinguished from chemisorption by considering the absolute value of ΔH°_{ads}. For physisorption processes, this magnitude is usually lower than 40 kJ mol^{-1} while that for chemisorptions approaches 100 kJ mol^{-1}.[65] In the present work, the absolute value of ΔH°_{ads} for adsorption of AHMT is 19.85 kJ mol^{-1}, which is lower than 40 kJ mol^{-1} and indicates that physisorption takes place. The negative sign of ΔH°_{ads} indicates that the adsorption of AHMT on the copper surface from 2 M HNO_3 solution is an exothermic process. The adsorption process of AHMT onto copper surface includes, at least, two steps: the adsorption of AHMT molecules onto copper surface and simultaneous desorption of some hydration water from the copper surface. The former process is expected to cause a decrease in randomness, thus in ΔS°_{ads}. The later process could cause some increase in disorderness. The obtained entropy value seems to be in contrast to that normally accepted in the adsorption phenomenon. While the adsorption of organic molecules is generally exothermic with decrease in entropy, the contrary occurs for the desorption of water molecules. The thermodynamic values obtained are the algebraic sum of those of the adsorption of organic molecules and desorption of water molecules. Therefore, the positive value of ΔS°_{ads} related to substitutional adsorption can be attributed to the increase in the solvent entropy and to more positive water desorption entropy.[66] The positive value of ΔS°_{ads} was also interpreted by the increase of disorder due to desorption of more water molecules from the metal surface by one inhibitor molecule.[67]

ΔH°_{ads} and ΔS°_{ads} for the adsorption of AHMT on copper surface can be also deduced from eq 11. Indeed, Figure 8 shows the plot of ΔG°_{ads} versus T which gives straight line with a slope of $-\Delta S^{\circ}_{ads}$ and intercept of ΔH°_{ads}. The calculated ΔH°_{ads} in this case is −19.84 kJ mol^{-1}, confirming the exothermic behavior of the AHMT adsorption on the copper surface. Values of ΔH°_{ads} obtained by the both methods are in good agreement. Moreover, the deduced ΔS°_{ads} value of 34.74 J mol^{-1} K^{-1} is very close to that obtained using the Van't Hoff equation (Table 6).

4. CONCLUSIONS

Purpald (AHMT) shows excellent inhibition properties for the corrosion of copper in 2 M HNO_3 at 303 K and the inhibition efficiency increases with increase in the inhibitor concentration. At 10^{-2} M. the inhibition efficiency, η(%) of AHMT obtained by using gravimetric method is as high as 91.7%. The inhibitor efficiencies determined by weight loss, ac impedance, and dc polarization methods are in reasonable agreement. On the basis of the Tafel polarization results, AHMT can be classified as mixed inhibitor. The η% of AHMT is found to decrease proportionally with increasing temperature and its addition to 2 M HNO_3 leads to decrease of apparent activation energy (E_a) of corrosion process. The corrosion process is inhibited by the adsorption of AHMT on copper surface and the adsorption of the inhibitor fits a Langmuir isotherm model under all of the studied temperatures. Thermodynamic adsorption parameters show that AHMT is adsorbed on copper surface by an exothermic spontaneous process. Moreover, the calculated values of ΔG°_{ads} and ΔH°_{ads} reveal that the adsorption mechanism of AHMT on copper surface in 2 M HNO_3 solution is mainly due to physisorption.

AUTHOR INFORMATION

Corresponding Author

*Phone.: +33 320 336 311. E-mail: fbentiss@gmail.com.

Notes

The authors declare no competing financial interest.

REFERENCES

(1) Zarrouk, A.; Dafali, A.; Hammouti, B.; Zarrok, H.; Boukhris, S.; Zertoubi, M. Synthesis, characterization and comparative study of functionalized quinoxaline derivatives towards corrosion of copper in nitric acid medium. *Int. J. Electrochem. Sci.* **2010**, *5*, 46−55.

(2) Zarrouk, A.; Chelfi, T.; Dafali, A.; Hammouti, B.; Al-Deyab, S. S.; Warad, I.; Benchat, N.; Zertoubi, M. Comparative study of new pyridazine derivatives towards corrosion of copper in nitric acid: part-1. *Int. J. Electrochem. Sci.* **2010**, *5*, 696−705.
(3) Zarrouk, A.; Warad, I.; Hammouti, B.; Dafali, A.; Al-Deyab, S. S.; Benchat, N. The effect of temperature on the corrosion of Cu/HNO_3 in the presence of organic inhibitor: part-2. *Int. J. Electrochem. Sci.* **2010**, *5*, 1516−1526.
(4) Zarrouk, A.; Hammouti, B.; Touzani, R.; Al-Deyab, S. S.; Zertoubi, M.; Dafali, A.; Elkadiri, S. Comparative study of new quinoxaline derivatives towards corrosion of copper in nitric acid. Int. *J. Electrochem. Sci.* **2011**, *6*, 4939−4952.
(5) Zarrouk, A.; Hammouti, B.; Dafali, A.; Zarrok, H. L-Cysteine methyl ester hydrochloride: A new corrosion inhibitor for copper in nitric acid. *Der Pharma Chem.* **2011**, *3* (4), 266−274.
(6) Zarrouk, A.; Hammouti, B.; Zarrok, H.; Warad, I.; Bouachrine, M. N-containing organic compound as an effective corrosion inhibitor for copper in 2M HNO_3: weight loss and quantum chemical study. *Der Pharma Chem.* **2011**, *3* (5), 263−271.
(7) Khaled, K. F. Experimental and atomistic simulation studies of corrosion inhibition of copper by a new benzotriazole derivative in acid medium. *Electrochim. Acta* **2009**, *54*, 4345−4352.
(8) Kosec, T.; Merl, D. K.; Milošev, I. Impedance and XPS study of benzotriazole films formed on copper. copper−zinc alloys and zinc in chloride solution. *Corros. Sci.* **2008**, *50*, 1987−1997.
(9) Sherif, E. M. Corrosion and corrosion inhibition of pure ion in neutral chloride solutions by 1,1′-thiocarbonyldiimidazole. *Int. J. Electrochem. Sci.* **2011**, *6*, 3077−3092.
(10) Sherif, E. M.; Park, S.-M. Effects of 2-amino-5-ethylthio-1,3,4-thiadiazole on copper corrosion as a corrosion inhibitor in aerated acidic pickling solutions. *Electrochim. Acta* **2006**, *51*, 6556−6562.
(11) Sherif, E. M.; Erasmus, R. M.; Comins, J. D. Inhibition of copper corrosion in acidic chloride pickling solutions by 5-(3-aminophenyl)-tetrazole as a corrosion inhibitor. *Corros. Sci.* **2008**, *50*, 3439−3445.
(12) Sherif, E. M. Effects of 2-amino-5-(ethylthio)-1,3,4-thiadiazole on copper corrosion as a corrosion inhibitor in 3% NaCl solutions. *J. Appl. Surf. Sci.* **2006**, *252*, 8615−8623.
(13) Sherif, E. M.; Almajid, A. A. Surface protection of copper in aerated 3.5% sodium chloride solutions by 3-amino-5-mercapto-1,2,4-triazole as a copper corrosion inhibitor. *J. Appl. Electrochem.* **2010**, *40*, 1555−1562.
(14) Sherif, E. M.; Erasmus, R. M.; Comins, J. D. Corrosion of copper in aerated acidic pickling solutions and its inhibition by 3-amino-1,2,4-triazole-5-thiol. *J. Colloid Interface Sci.* **2007**, *306*, 96−104.
(15) Sherif, E. M.; Erasmus, R. M.; Comins, J. D. Effects of 3-amino-1,2,4-triazole on the inhibition of copper corrosion in acidic chloride solutions. *J. Colloid Interface Sci.* **2007**, *311*, 144−151.
(16) Sherif, E. M. Electrochemical and gravimetric study on the corrosion and corrosion inhibition of pure copper in sodium chloride solutions by two azole derivatives. *Int. J. Electrochem. Sci.* **2012**, *7*, 1482−1495.
(17) Sherif, E. M. Corrosion behavior of copper in 0.5 M hydrochloric acid pickling solutions and its inhibition by 3-amino-1,2,4-triazole and 3-amino-5-mercapto-1,2,4-triazole. *Int. J. Electrochem. Sci.* **2012**, *7*, 1884−1897.
(18) Mihit, M.; Laarej, K.; Abou El Makarim, H.; Bazzi, L.; Salghi, R.; Hammouti, B. Study of the inhibition of the corrosion of copper and zinc in HNO_3 solution by electrochemical technique and quantum chemical calculations. *Arab. J. Chem.* **2010**, *3*, 55−60.
(19) Khaled, K. F.; Fadl-Allah, S. A.; Hammouti, B. Some benzotriazole derivatives as corrosion inhibitors for copper in acidic medium: Experimental and quantum chemical molecular dynamics approach. *Mater. Chem. Phys.* **2009**, *117*, 148−155.
(20) Khaled, K. F.; Amin, M. A. Dry and wet lab studies for some benzotriazole derivatives as possible corrosion inhibitors for copper in 1.0 M HNO_3. *Corros. Sci.* **2009**, *51*, 2098−2106.
(21) Antonijević, M. M.; Milić, S. M.; Petrović, M. B. Films formed on copper surface in chloride media in the presence of azoles. *Corros. Sci.* **2009**, *51*, 1228−1237.
(22) Lalitha, A.; Ramesh, S.; Rajeswari, S. Surface protection of copper in acid medium by azoles and surfactants. *Electrochim. Acta* **2005**, *51*, 47−55.
(23) Riggs, O. L., Jr. *Corrosion Inhibitors*, second ed.; C.C. Nathan: Houston, TX, 1973.
(24) Zarrouk, A.; Hammouti, B.; Zarrok, H.; Bouachrine, M.; Khaled, K. F.; Al-Deyab, S. S. Corrosion inhibition of copper in nitric acid solutions using a new triazole derivative. *Int. J. Electrochem. Sci.* **2012**, *7*, 89−105.
(25) Zarrouk, A.; Hammouti, B.; Al-Deyab, S. S.; Salghi, R.; Zarrok, H.; Jama, C.; Bentiss, F. Corrosion inhibition performance of 3,5-diamino-1,2,4-triazole for protection of copper in nitric acid solution. *Int. J. Electrochem. Sci.* **2012**, *7*, 5997−6011.
(26) Ahamad, I.; Prasad, R.; Quraishi, M. A. Thermodynamic, electrochemical and quantum chemical investigation of some Schiff bases as corrosion inhibitors for mild steel in hydrochloric acid solutions. *Corros. Sci.* **2010**, *52*, 933−942.
(27) Bentiss, F.; Outirite, M.; Traisnel, M.; Vezin, H.; Lagrenée, M.; Hammouti, B.; Al-Deyab, S. S.; Jama, C. Improvement of corrosion resistance of carbon steel in hydrochloric acid medium by 3,6-bis(3-pyridyl)pyridazine. *Int. J. Electrochem. Sci.* **2012**, *7*, 1699−1723.
(28) Matsumoto, F.; Ozaki, M.; Inatomi, Y.; Paulson, S. C.; Oyama, N. Studies on the adsorption behavior of 2,5-dimercapto-1,3,4-thiadiazole and 2-mercapto-5-methyl-1,3,4-thiadiazole at gold and copper electrode surfaces. *Langmuir* **1999**, *15*, 857−865.
(29) Bussolotti, F.; D'Addato, S.; Allegretti, F.; Dhanak, V.; Mariani, C. Molecular orientation of 2-mercaptobenzoxazole adsorbed on Cu(1 0 0) surface. *Surf. Sci.* **2005**, *578*, 136−141.
(30) Castro, V. D.; Bussolotti, F.; Mariani, C. The evolution of benzenethiol self-assembled monolayer on the Cu(1 0 0) surface. *Surf. Sci.* **2005**, *598*, 218−225.
(31) Lagrenée, M.; Mernari, B.; Bouanis, M.; Traisnel, M.; Bentiss, F. Study of the mechanism and inhibiting efficiency of 3,5-bis(4-methylthiophenyl)-4H-1,2,4-triazole on mild steel corrosion in acidic media. *Corros. Sci.* **2002**, *44*, 573−588.
(32) Ma, H.; Chen, S.; Zhao, S.; Liu, X.; Liu, D.; Li, D. A study of corrosion behavior of copper in acidic solutions containing cetyltrimethylammonium bromide. *J. Electrochem. Soc.* **2011**, *48*, B482−B488.
(33) Barcia, O. E.; Mattos, O. R.; Pebere, N.; Tribollet, B. Mass-Transport Study for the electrodissolution of copper in 1M hydrochloric acid solution by impedance. *J. Electrochem. Soc.* **1993**, *140*, 2825−2832.
(34) Binkley, J. S.; Pople, J. A.; Hehre, W. J. Self-consistent molecular orbital methods. 21. Small split-valence basis sets for first-row elements. *J. Am. Chem. Soc.* **1980**, *102*, 939−947.
(35) Lee, H. P; Nobe, K. Kinetics and mechanisms of Cu electrodissolution in chloride media. *J. Electrochem. Soc.* **1986**, *133*, 2035−2043.
(36) Ashassi-Sorkhabi, H.; Ghalebsaz-Jeddi, N.; Hashemzadeh, F.; Jahani, H. Corrosion inhibition of carbon steel in hydrochloric acid by some polyethylene glycols. *Electrochim. Acta* **2006**, *51*, 3848−3854.
(37) Goncalves, R. S.; Azambuja, D. S.; Serpa Lucho, A. M. Electrochemical studies of propargyl alcohol as corrosion inhibitor for nickel, copper, and copper/nickel (55/45) alloy. *Corros. Sci.* **2002**, *44*, 467−479.
(38) Solmaz, R.; Kardaş, G.; Çulha, M.; Yazıcı, B.; Erbil, M. Investigation of adsorption and inhibitive effect of 2-mercaptothiazoline on corrosion of mild steel in hydrochloric acid media. *Electrochim. Acta* **2010**, *53*, 5941−5952.
(39) Tsuru, T.; Haruyama, S. Corrosion monitor based on impedance method. II. Construction and its application to homogeneous corrosion. *J. Jpn. Soc. Corros. Eng.* **1978**, *27*, 573−579.
(40) Khaled, K. F. Corrosion control of copper in nitric acid Solutions using some amino acids − A combined experimental and theoretical study. *Corros. Sci.* **2010**, *52*, 3225−3234.
(41) Abd EI-Rehim, S. S.; Ibrahim, M. A. M.; Khaled, K. F. 4-Aminoantipyrine as an inhibitor of mild steel corrosion in HCl solution. *J. Appl. Electrochem.* **1999**, *29*, 593−599.

(42) Bouklah, M.; Benchat, N.; Aouniti, A.; Hammouti, B.; Benkaddour, M.; Lagrenée, M.; Vezin, H.; Bentiss, F. Effect of the substitution of an oxygen atom by sulphur in a pyridazinic molecule towards inhibition of corrosion of steel in 0.5M H_2SO_4 medium. *Prog. Org. Coat.* **2004**, *51*, 118−124.
(43) Smyrl, W. H. Electrochemistry and corrosion on homogeneous and heterogeneous metal surface. In *Comprehensive treatise of electrochemistry*; Bockris, J. O.; Conway, B., Yager, E., White, R. E., Eds.; Plenum Press: New York, London, 1981; Vol. *4*, p 97.
(44) Bentiss, F.; Lebrini, M.; Lagrenée, M. Thermodynamic characterization of metal dissolution and inhibitor adsorption processes in mild steel/2,5-bis(*n*-thienyl)-1,3,4-thiadiazoles/hydrochloric acid system. *Corros. Sci.* **2005**, *47*, 2915−2931.
(45) Herrag, L.; Hammouti, B.; Elkadiri, S.; Aouniti, A.; Jama, C.; Vezin, H.; Bentiss, F. Adsorption Properties and Inhibition of mild steel corrosion in hydrochloric solution by some newly synthesized diamine derivatives: experimental and theoretical investigations. *Corros. Sci.* **2010**, *52*, 3042−3051.
(46) Riggs, O. L., Jr.; Hurd, R. M. Temperature coefficient of corrosion inhibition. *Corrosion* **1967**, *23*, 252−258.
(47) Fouda, A. S.; Al-Sarawy, A. A.; El-Katori, E. E. Pyrazolone derivatives as corrosion inhibitors for C-steel in hydrochloric acid solution. *Desalination* **2006**, *201*, 1−3.
(48) Szauer, T.; Brand, A. Adsorption of oleates of various amines on iron in acidic solution. *Electrochim. Acta* **1981**, *26*, 1253−1256.
(49) Solmaz, R.; Kardaş, G.; Çulha, M.; Yazıcı, B.; Erbil, M. Investigation of adsorption and inhibitive effect of 2-mercaptothiazoline on corrosion of mild steel in hydrochloric acid media. *Electrochim. Acta* **2008**, *53*, 5941−5952.
(50) Solmaz, R.; Kardaş, G.; Yazıcı, B.; Erbil, M. Adsorption and corrosion inhibitive properties of 2-amino-5-mercapto-1,3,4-thiadiazole on mild steel in hydrochloric acid media. *Colloids Surf. A Physicochem. Eng. Aspects* **2008**, *312*, 7−17.
(51) Guan, N. M.; Xueming, L.; Fei, L. Synergistic inhibition between *o*-phenanthroline and chloride ion on cold rolled steel corrosion in phosphoric acid. *Mater. Chem. Phys.* **2004**, *86*, 59−68.
(52) Abd El Rehim, S. S.; Ibrahim, M. A. M.; Khalid, K. F. The inhibition of 4-(2′-amino-5′-methylphenylazo) antipyrine on corrosion of mild steel in HCl solution. *Mater. Chem. Phys.* **2001**, *70*, 268−273.
(53) Gomma, M. K.; Wahdan, M. H. Schiff bases as corrosion inhibitors for aluminium in hydrochloric acid solution. *Mater. Chem. Phys.* **1995**, *39*, 209−213.
(54) Sahin, M.; Bilgic, S.; Yilmaz, H. The inhibition effects of some cyclic nitrogen compounds on the corrosion of the steel in NaCl mediums. *Appl. Surf. Sci.* **2002**, *195*, 1−4.
(55) Ateya, B.; El-Anadouli, B. E.; El-Nizamy, F. M. The adsorption of thiourea on mild steel. *Corros. Sci.* **1984**, *24*, 509−515.
(56) Labjar, N.; Lebrini, M.; Bentiss, F.; Chihib, N.-E.; El Hajjaji, S.; Jama, C. Corrosion inhibition of carbon steel and antibacterial properties of aminotris-(methylenephosphonic) acid. *Mater. Chem. Phys.* **2010**, *119*, 330−336.
(57) Bentiss, F.; Lebrini, M.; Lagrenée, M.; Traisnel, M.; Elfarouk, A.; Vezin, H. The influence of some new 2,5-disubstituted 1,3,4-thiadiazoles on the corrosion behaviour of mild steel in 1 M HCl solution: AC impedance study and theoretical approach. *Electrochim. Acta* **2007**, *52*, 6865−6872.
(58) Tang, L.; Li, X.; Lin, L.; Mu, G.; Liu, G. The effect of 1-(2-pyridylazo)-2-naphthol on the corrosion of cold rolled steel in acid media: Part 2: Inhibitive action in 0.5 M sulfuric acid. *Mater. Chem. Phys.* **2006**, *97*, 301−307.
(59) Tebbji, K.; Faska, N.; Tounsi, A.; Ouddad, H.; Benkaddour, M.; Hammouti, B. The effect of some lactones as inhibitors for the corrosion of mild steel in 1 M hydrochloric acid. *Mater. Chem. Phys.* **2007**, *106*, 260−267.
(60) Mu, G.; Li, X.; Liu, G. Synergistic inhibition between tween 60 and NaCl on the corrosion of cold rolled steel in 0.5 M sulfuric acid. *Corros. Sci.* **2005**, *47*, 1932−1952.
(61) Outirite, M.; Lagrenée, M.; Lebrini, M.; Traisnel, M.; Jama, C.; Vezin, H.; Bentiss, F. Ac impedance, X-ray photoelectron spectroscopy and density functional theory studies of 3,5-bis(*n*-pyridyl)-1,2,4-oxadiazoles as efficient corrosion inhibitors for carbon steel surface in hydrochloric acid solution. *Electrochim. Acta* **2010**, *55*, 1670−1681.
(62) Ali, S. A.; Al-Muallem, H. A.; Saeed, M. T.; Rahman, S. U. Hydrophobic-tailed bicycloisoxazolidines: A comparative study of the newly synthesized compounds on the inhibition of mild steel corrosion in hydrochloric and sulfuric acid media. *Corros. Sci.* **2008**, *50*, 664−675.
(63) Bentiss, F.; Triasnel, M.; Lagrenée, M. The substituted 1,3,4-oxadiazoles: a new class of corrosion inhibitors of mild steel in acidic media. *Corros. Sci.* **2000**, *42*, 127−146.
(64) Bouklah, M.; Hammouti, B.; Lagrenée, M.; Bentiss, F. Thermodynamic properties of 2,5-bis(4-methoxyphenyl)-1,3,4-oxadiazole as a corrosion inhibitor for mild steel in normal sulfuric acid medium. *Corros. Sci.* **2006**, *48*, 2831−2842.
(65) Noor, E. A.; Al-Moubaraki, A. H. Thermodynamic study of metal corrosion and inhibitor adsorption processes in mild steel/1-methyl-4[4′(-X)-styryl pyridinium iodides/hydrochloric acid systems. *Mater. Chem. Phys.* **2008**, *110*, 145−154.
(66) Branzoi, V.; Branzoi, F.; Baibarac, M. The inhibition of the corrosion of Armco iron in HCl solutions in the presence of surfactants of the type of *N*-alkyl quaternary ammonium salts. *Mater. Chem. Phys.* **2000**, *65*, 288−297.
(67) Saleh, M. M. Inhibition of mild steel corrosion by hexadecylpyridinium bromide in 0.5M H_2SO_4. *Mater. Chem. Phys.* **2006**, *98*, 83−89.